

SEISMIC BEHAVIORS AND EVALUAION OF REINFORCED CONCRETE WALLS REINFORCED BY SBPDN REBARS.

Chuxuan Wei*¹, Yuping Sun*², Takashi Takeuchi*³, Takao Nakagawa*⁴

ABSTRACT

Three concrete walls, whose longitudinal distributed bars were not anchored into adjacent beams, were fabricated and tested under cyclic lateral load to investigate the effectiveness of a new arrangement of longitudinal bars in wall panel as well as the influence of shear span ratio on seismic behaviors of the walls reinforced by SBPDN rebars. The test results indicated that all walls exhibited drift-hardening behavior till drift ratio of 3%. Furthermore, an analytic method that can take account of the slippage of SBPDN rebars was presented to discuss the influence of arrangement of longitudinal bars.

Keywords: SBPDN rebar, RC wall, shear span ratio, longitudinal rebar, drift-hardening capability

1. INTRODUCTION

Reinforced concrete (RC) walls have been widely applied in earthquake-resistant structural systems. However, due to their high lateral stiffness, RC walls tend to attract large amount of seismic energy and hence to resist large earthquake-induced lateral loads, causing severe damages that concentrate at the wall toes and are generally very difficult to be repaired. The utilization of longitudinal rebars concentrated at the edge zones of shear walls can enhance the flexure resistance of shear walls without boundary columns, and Fujitani et al. [1] have experimentally verified that using the weakly bonded ultra-high strength rebar (referred to as SBPDN rebar) could reduce residual deformation of RC walls, and keep increasing the lateral resistance of the walls until large drift level, which is hereafter referred to as drift-hardening capability. However, the previous study by Fujitani et al [1] also confirmed that because the flexure strength of the walls can be greatly enhanced by SBPDN rebars, brittle shear failure is more likely to occur if the shear reinforcement is not sufficient.

To avoid premature shear failure of RC walls with SBPDN rebars, this paper proposes a new arrangement of longitudinal distributed (LD) bars in the wall panel. The LD bars are not anchored into the adjacent beams so

bending moment and reduce the flexural strength of the walls. This method is also expected to delay the local buckling of LD bars, mitigate the damage of concrete near the wall toes, and prevent shear failure of RC walls with SBPDN rebars and shorter shear span.

The primary objectives of this paper are to verify the effectiveness of the new arrangement method for LD rebars in the wall panel and to investigate the influence of shear span ratio (a/D) on seismic behavior of the RC walls reinforced by SBPDN rebars. Furthermore, an analytical method is presented to take account of the effect of slippage of SBPDN rebars and is verified by comparing with the test results.

2. EXPERIMENTAL PROGRAMS

2.1 Outlines of the specimens

To achieve the aforementioned goals, three 1/3-scale cantilever rectangular RC walls were fabricated and tested under reversed cyclic lateral loading while subjected to constant axial load. Fig. 1 shows the dimensions and reinforcement details of the specimens, while Table 1 lists the primary experimental parameters along with the main test results. As obvious from Table 1 and Fig. 1, all specimens have identical cross section. Each specimen has a rectangular section of 150mm in

Table 1 Primary experimental parameters and main test results

Specimen	h (mm)	a/D	n	f'_c (N/mm ²)	Longitudinal rebars		Concentrated SBPDN rebars		Transverse rebars		Q_{exp} (kN)
					Type	$\rho_{lv}(\%)$	Type	$\rho_s(\%)$	Type	$\rho_{wh}(\%)$	
W15	700	1.5	0.073	33.9	20-D6	0.70	8-U12.6	0.58	D6@65	0.65	329.1
W20	1000	2.0		36.0							252.6
W25	1300	2.5		35.8							191.2

h : clear height of wall panel; a/D : shear span ratio; n : axial load ratio; f'_c : concrete cylinder strength; ρ : reinforcement ratio; Q_{exp} : measured maximum lateral force; that they do not directly resist the axial stress caused by

- *1 Ph.D. Student, Graduate School of Engineering, Kobe University, JCI Student Member
- *2 Professor, Graduate School of Engineering, Kobe University, JCI Member
- *3 Assistant Professor, Graduate School of Engineering, Kobe University, JCI Member
- *4 Graduate Student, Graduate School of Engineering, Kobe University, JCI Student Member

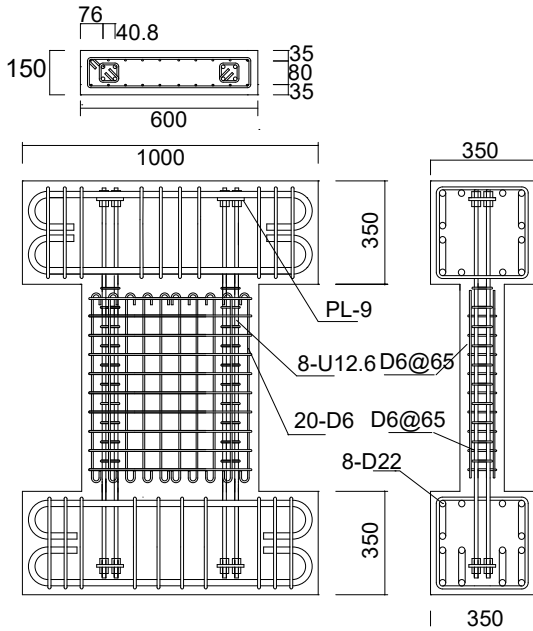


Fig.1 Dimensions and reinforcement details (unit: mm)

Table 2 Mechanical properties of the steels

Type		f_y N/mm ²	ϵ_y ×0.01	f_u N/mm ²	E_s kN/mm ²
D6	SD295A	402	0.21	524	192
U12.6	SBPDN 1275/1420	1394	0.84	1467	217

f_y : yield stress; f_u : ultimate stress; E_s : Young's modulus; ϵ_y : yield strain (0.2% offset strain);

thickness and 600mm in depth. The steel amount of LD bars and horizontal distributed (HD) bars in wall panel as well as of SBPDN rebars is the same for all test walls. The LD bars consisted of twenty D6 deformed bars uniformly placed with a spacing of 59 mm to give a steel ratio of 0.70%, while the HD bars were comprised of D6 deformed bars with a spacing of 65 mm. The LD bars were anchored at wall ends with 180-degree hooks as shown in Fig. 1, and the HD bars were placed in a closed form to sustain shear force and provide effective confinement effect. Eight SBPDN rebars with nominal diameter of 12.6mm were placed at the edge zones of wall panel. The mechanical properties of the steels used are listed in Table 2. Ready mixed concrete made of Portland cement and coarse aggregates with maximum diameter of 20 mm was used to fabricate the specimens. The target concrete strength was 30MPa, and the axial load ratio was 0.073 for all specimens.

The experimental variable was shear span ratio. To be specific, the specimen W15 had a shear span of 900 mm was to give a shear span ratio of 1.5. As for specimens W20 and W25, their shear spans were 1200 mm and 1500 mm, respectively, to give shear span ratios of 2.0 and 2.5, respectively.

2.2 Test program and loading program

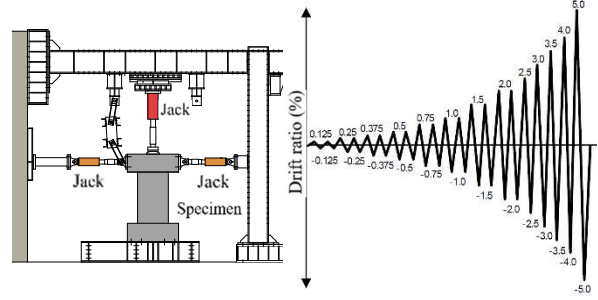
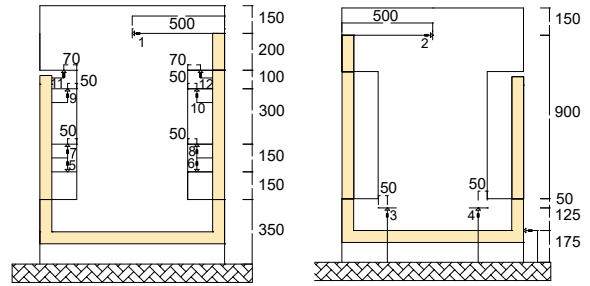


Fig.2 Schematic view of test apparatus

Fig.3 Loading program of test apparatus



(a) North (b) South
Fig.4 Location of displacement transducers (DTs) (unit: mm)

The experiments were conducted using the setup shown in Fig. 2. The loading apparatus was designed to subject the shear wall to reversed cyclic lateral load and constant axial compression. A vertical hydraulic jack with a capacity of 1000 kN, which was connected to stiff loading frame via a roller, was used to apply constant axial compression. The reversed cyclic lateral load was applied by two 500 kN horizontal hydraulic jacks. The lateral loading was controlled by drift ratio (R), which is defined as the ratio of the lateral displacement at the loading point of lateral force (Δ) to the shear span (a) of each shear wall. The loading program is shown in Fig. 3. Two complete cycles were applied at each level of targeted drifts till drift ratio reached 2%, and one cycle was applied at each level of targeted drift after drift ratio was beyond 2%.

Fig. 4 shows the locations of displacement transducers (DTs) of specimen W15 as an example. As shown in Fig. 4, two DTs were installed to measure the lateral displacement, and the average value measured by DTs No.1 and 2 were used as the lateral displacement of specimen. The other eight (four pairs of) DTs were installed to measure the local vertical displacement at several targeted heights of specimens. DTs No.1 through No.10 were also installed to specimens W20 and W25 in the same way as in specimen W15, and two more DTs, DT No.11 and 12, were set at the height of 1000 mm away from the wall base of W20 to measure the vertical displacement at that height, while two more pairs of DTs located at 900 mm and 1300 mm away from bottom stub of W25 were installed separately to measure relative vertical displacement. Besides, a total of 29 strain gauges were embedded to measure the axial strains of SBPDN rebars.

3. OBSERVED BEHAVIORS AND RESULTS

3.1 Cracks and damages of specimens

Fig. 5 shows the developments of cracks that were observed from web side of each specimen. In Fig. 5, the grids have a spacing of 50 mm, the red lines and blue lines represent the cracks that were drawn at the peak drifts of 0.75%, 1.5%, and 3.0% in both push and pull direction of lateral loading, respectively, while the blacked portions express the spalled-off concrete.

For specimen W15, the first flexure crack was confirmed at the boundary between the bottom loading beam and wall panel when the lateral force was 40kN. Accompanying with the development of the flexure crack at position of 120 mm from the wall base, the first flexure-shear crack was found when drift ratio reached 0.125%. Then, the initial spalling of concrete was observed when drift ratio reached 1%. Significant spalling-off of concrete along with the exposure of the LD bars were first confirmed at the drift ratio of 2.5%. The shear crack that located at 480 mm away from base run through north (web) surface of specimen when drift ratio reached 3.5%, accompanied with degradation of the lateral resistance and exposure of the HD bars in the wall panel was confirmed. After reaching the peak point in pull direction at the drift ratio of -4%, obvious expansion of flexure and shear cracks were observed, and the test was terminated at that drift level.

For specimen W20, the first flexure crack was confirmed at boundary between the bottom loading beam and wall panel at the drift ratio of 0.125%. The first shear crack was found when drift ratio reached 0.375%. The initial spalling-off of concrete was observed at drift ratio of 2%, and obvious spalling-off of the concrete as well as exposure of the HD bars were first confirmed when drift ratio reached 2.5%. At the drift ratio of 3.5%, shear crack that located at 280mm away from base run through north (web) surface of the specimen.

As for specimen W25, the first flexure crack was confirmed at boundary between the bottom loading beam and the wall panel at the drift ratio of 0.125%. Accompanying with the development of the flexure crack at position of 240 mm from the bottom loading beam, the first flexure-shear crack was found when drift ration reached 0.25%. When drift ratio reached 1.5%, the initial spalling-off of concrete at the extreme corner of wall panel was confirmed and spalling-off of concrete became significant at from the drift ratio of 2.5% on.

For all three specimens, no local buckling of the LD bars in the wall panel was observed. As compared with the previous results [1], because the LD bars were not anchored into the top and bottom beams, they tended to sustain less lateral loading and absorb less energy, and hence mitigate damages near the wall toes. On the other hand, this new arrangement of LD bars might reduce the shear reinforcements of the bottom loading beam, and damage the loading beam adjacent to the wall toes. As shown in Fig. 6, severe damages at the panel-beam joint were observed for all three specimens. This fact implies that the adjacent members should be stiff enough to take full advantage of the new arrangement method.

In the specimen with shear span ratio of 1.5, the

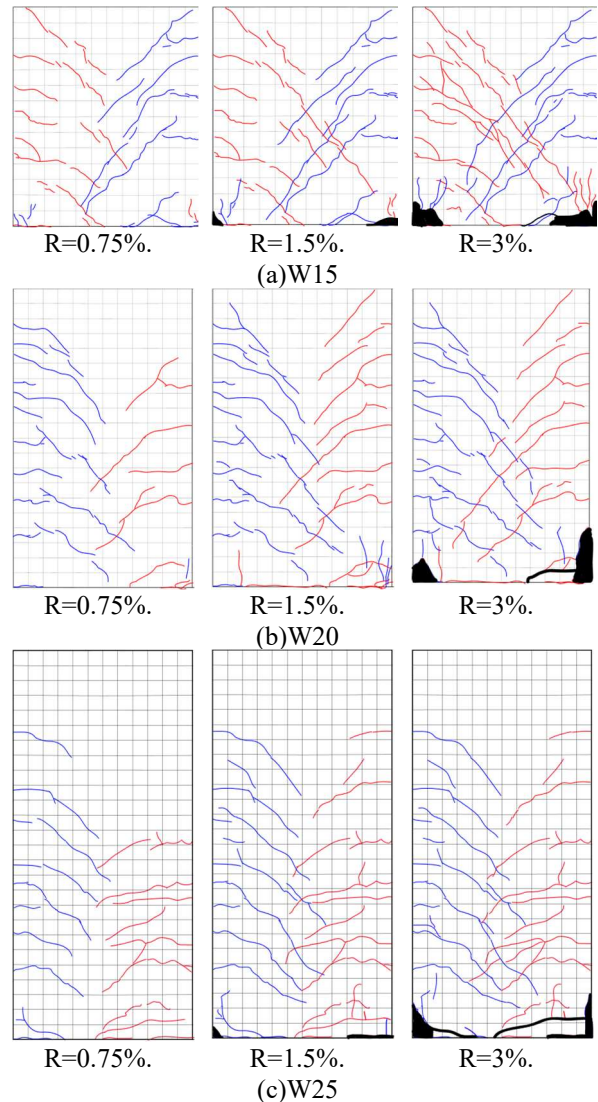


Fig.5 Cracks patterns observed on specimens



Fig.6 Damage at beam-wall joint (specimen W15 at the loading cycle of 4%)

flexure cracks were spread about 600 mm upper from the wall base, while for specimens with shear span ratio of 2.0 and 2.5, the flexure cracks were spread about 875 mm and 1050 mm in height, respectively. Distribution of the flexural cracks implies that the length of plastic hinge region (details can be found in section 3.4) of RC walls should be associated with the shear span of them.

3.2 Hysteretic behaviors

Fig. 7 shows the measured lateral load versus drift ratio relationships, while the measured lateral capacities averaging the peak lateral forces in both directions are shown in Table 1. As shown in Fig. 7, the lateral resistances of specimens W15, W20 and W25 all stably

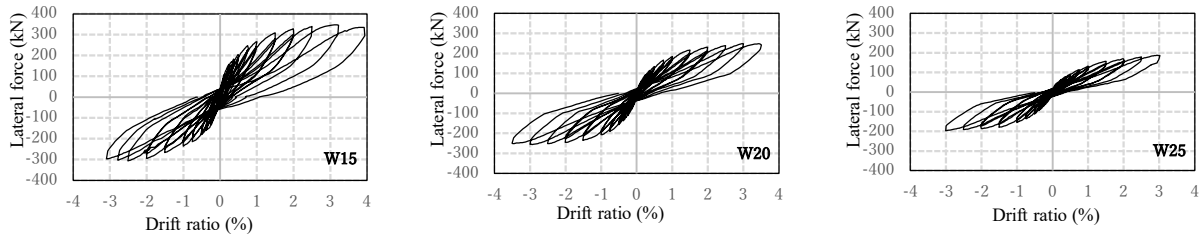


Fig.7 Measured lateral load-drift ratio relationships

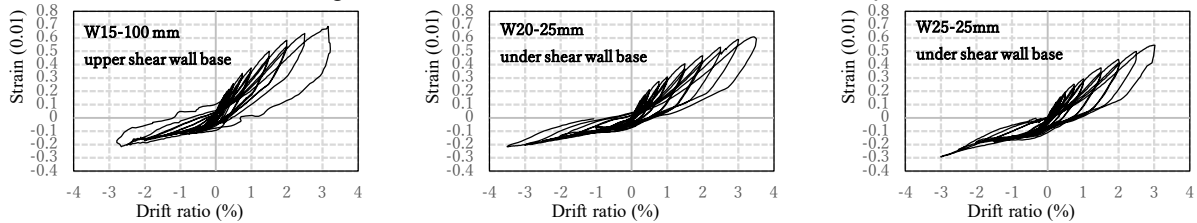


Fig.8 Measured strains-drift ratio relationships of SBPDN rebars

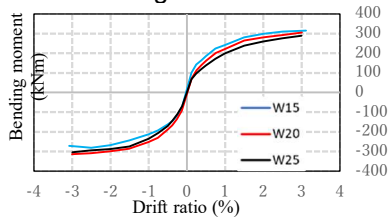


Fig.9 Comparison of Flexural strengths of the wall sections

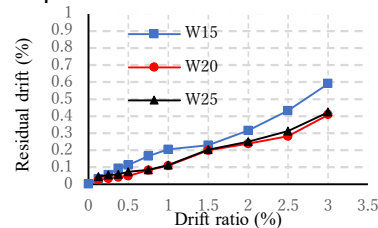


Fig.10 Measured residual drift ratios

increased along with drift, and all specimens exhibited drift-hardening capability up to the drift level of 3.0% regardless of the difference in shear span ratio.

The lateral resistance forces of specimens W15 and W20 reached peaks at $R = 3.0\%$ and decreased slightly at $R = 3.5\%$. As for specimen W25, due to the limitation in the stroke length of the horizontal loading jacks, the cyclical loading was terminated after the cycle at $R = 3.0\%$.

Fig.8 displays the measured axial strain versus drift ratio relationships of the SBPDN rebars placed in the initial tensional edge zone for each specimen. The strains shown in Fig.8 represent those measured by the strain gauges located at the section of 25mm away from the wall base for specimens W20 and W25, while that of specimen W15 was the strain measured at the section 100 away from the wall base because the data at the 25mm section could not experimentally obtained. It is apparent from Fig.8 that the axial strain of SBPDN rebars exhibited stable increase along with the drift ratio, and did not reach its yield strain (0.84%) till the end of loading. This observation means that SBPDN rebars could provide lateral resistance even after the significant spalling of cover concrete had commenced (see Fig.5.)

In order to ascertain the ultimate failure state of the walls reinforced with SBPDN rebars, after the reversed cycling of lateral load, all specimens were monotonically pushed up to the drift level of 7.0%. Although severe damage at the wall toes was confirmed (see Fig.6), and the lateral resistance decreased along with drift ratio due to the increasing of $P-\Delta$ effect, all specimens still maintained more than 60% of the maximum lateral force till the end of tests at $R = 7.0\%$ without losing their gravity-sustaining capacity.

To see the influence of shear span ratio on seismic behavior of the tested shear walls, comparisons were conducted in terms of the moment at the end section versus drift ratio envelope curves and shown in Fig.9. It can be seen from Fig.9 that there is little, in any, difference among the flexural strength of these three specimens, implying that influence of shear span ratio on flexural property of the wall section can be ignored.

3.3 Residual drift ratios

Fig.10 shows the average residual drift ratio in the push and pull directions measured at each drift level. The test results indicated that the residual drift ratios of RC walls reinforced by SBPDN rebars could be kept below 0.4% - 0.6% after being unloaded at $R = 3.0\%$.

3.4 Proportion of various deformation and length of potential plastic hinge region

To calculate the proportion of flexure and shear deformation and the length of potential plastic hinge region from the experimental data, it is assumed that the overall deformation of the walls (Δ) consists of only flexure (Δ_f) and shear (Δ_s) deformation, and that the curvature concentrates in the potential plastic hinge region as a constant and the curvature outside the hinge region is neglected. Based on these two assumptions, the measured proportion of flexural deformation α and the length of potential plastic hinge region L_p ($L_p = \beta * D$, D is the depth of the wall panel (600 mm)) can be calculated by using the procedures proposed by Fukuhara et al [2].

Considering that the vertical displacements measured by DTs No. 3 through No. 10 (see Fig. 4) might be not reliable when the drift ratio was larger than 1.5% due to the spalling of cover concrete, only the

Table 3 Proportion of flexural deformation α

Drift ratio (%)	0.125	0.25	0.375	0.5	0.75	1	1.5	average
W15	0.61	0.63	0.71	0.71	0.73	0.71	0.71	0.69
W20	0.80	0.80	0.83	0.85	0.82	0.81	0.84	0.83
W25	0.87	0.73	0.78	0.81	0.82	0.82	0.86	0.82

Table 4 The factor of measured potential plastic hinge region β

Drift ratio (%)	0.125	0.25	0.375	0.5	0.75	1	1.5	average
W15	1.13	0.68	0.34	0.32	0.30	0.28	0.27	0.45
W20	0.64	0.64	0.58	0.58	0.37	0.35	0.31	0.47
W25	1.16	1.12	0.84	0.73	0.66	0.36	0.32	0.69

Table 5 Comparison of ultimate capacities

Specimen	Q_{mu1} (kN)	Q_{mu2} (kN)	Q_{su} (kN)	Q_{exp} (kN)	$Q_{exp}/$ Q_{mu2}	$Q_{su}/$ Q_{mu2}
W15	486	374	306	329	0.88	0.82
W20	368	284	288	253	0.89	1.01
W25	294	228	272	191	0.84	1.20

Q_{mu1} : Calculated ultimate flexural strength by Eq.1
 Q_{mu2} : Ultimate flexural strength calculated by NewRC block
 Q_{su} : Calculated ultimate shear strength by Eq.2
 Q_{exp} : Measured maximum lateral force

calculated results of α and β until the drift ratio of 1.5% are shown in Table 3 and Table 4, respectively. It was found that the larger the shear span ratio, the larger the proportion of flexural deformation and the longer the length of potential plastic hinge region.

4. ANALYSIS AND DISCUSSION

4.1 Evaluation of ultimate capacities

At first, Eq.1 and Eq.2 recommended by the current standard of Japan [3] are used to calculate the ultimate flexural and shear strengths, respectively.

$$Q_{mu1} = (a_{pt}\sigma_{py}l_w + 0.5a_w\sigma_{wy} + 0.5Nl_w)/a \quad (1)$$

$$Q_{su} = \left\{ \frac{0.068p_{te}^{0.23}(f'_c+18)}{\sqrt{a/D+0.12}} + 0.85\sqrt{p_{wh}\sigma_{hy}} + 0.1\sigma_0 \right\} bj \quad (2)$$

Because the D6 LD bars in wall panel were not anchored into the adjacent loading beams, they are assumed not to sustain axial stress induced by bending moment when calculating the flexural strength by Eq. 1. The calculated ultimate capacities are compared with the experimental results in Table 5. It is obvious from Table 5 that Eq.1 overestimates the flexure strength of RC walls reinforced with SBPDN rebars by 46% -54 %, because SBPDN rebars did not yield until $R = 3.0$ %.

The flexural strength calculated using the NewRC block method [4] and is assumed that the cross sections remain plane and the rebars are perfectly bonded with concrete, which has been recommended for the concrete components made of high-strength materials, is also compared with the experimental ultimate capacities in Table 5. One can see from Table 5 that the calculated flexural strengths by NewRC block

agreed much better with the test results than those calculated by Eq. 1, but they still overestimate the flexure strength by 11% - 16% because it ignores the effect of the slippage of SBPDN rebars. As for the ultimate shear strength, since no shear failure was observed in all specimens till drift ratio of 3%, it can be presumed that Eq.2 underestimates the shear strength of specimen W15 with shear span ratio of 1.5. It is worthy noted that the ratio of Q_{su} to Q_{mu2} (see Table 5) well predicts the failure mode of specimens W20 and W25.

4.2 Refined evaluation of ultimate capacities

To promote the application of RC walls reinforced by SBPDN rebars to actual buildings, it is indispensable to develop a refined method to evaluate the ultimate capacities of the walls reasonably and accurately.

To reasonably evaluate the seismic behavior, both shear and flexure strength, of RC walls reinforced by SBPDN rebars, the analytical method that can take account of the effect of slippage of SBPDN rebars in RC columns proposed by Funato et al [5], and the evaluation method of ultimate shear strength for concrete columns recommended in the design guidelines of AIJ [6], which can consider the degradation of shear strength along with the drift will be adopted in this paper.

When utilizing the method [5] to evaluate the overall seismic behavior of RC walls reinforced with SBPDN rebars, the following assumptions are made: 1) concrete does not resist tensile stress, 2) the concrete plane remains plane after bending, 3) NewRC model [4] is used to define the stress-strain relation of concrete, 4) the stress-strain relation of D6 bar is completely elastic-plastic model, while Menegotto-Pinto model is utilized for SBPDN rebars, 5) the bond-slip relationship of the SBPDN rebar follows the model developed by Funato et al [5] with a bond strength of 3 N/mm², 6) the proportion of flexure deformation is given by the results shown in Table 3, the length of the potential plastic hinge region is determined and based on the test results shown in Table 4, and the average values of α and β were used in the calculation.

Fig. 11 compares the measured results with the calculated ones in terms of envelopes of hysteretic responses and the residual drift ratios. To investigate the influence of the D6 LD bars in the wall panel, two calculated envelopes are shown in Fig. 11. The red lines represent the results where the D6 LD bars are neglected while the blue lines express the calculated results with the D6 LD bars being fully taken into consideration.

From Fig. 11(a) one can see that at the initial stage of loading, the calculated envelopes in red lines exhibit better agreement with the experimental curves than the blue lines, which implies that the LD bars in the wall did not directly sustain the axial stress induced by bending moment as expected. However, as the drift ratio increases, the calculated envelopes in blue lines trace the experimental curves very well up to the drift of 3.0 %, implying that the LD bars near the edge zone of the wall section will sustain axial compressive stress induced by bending moment at large deformation.

It is also obvious from Fig. 11(b) that complete ignorance of the D6 LD bars tends to underestimate the

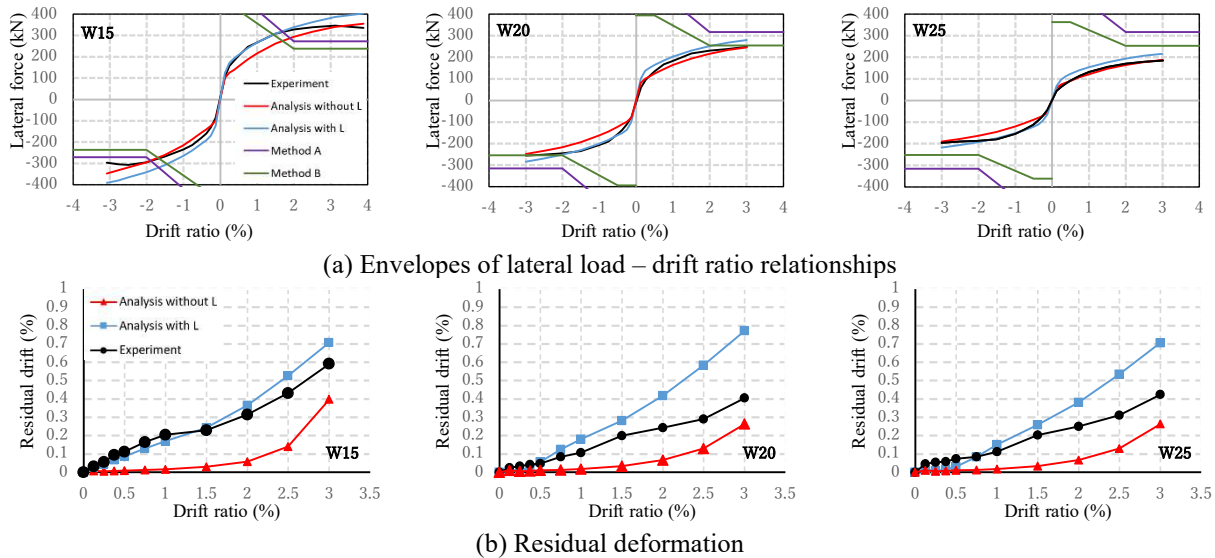


Fig.11 Comparisons between measured and analytical results

residual deformation, while full consideration of the LD bars overestimates the test result. These observations indicate that to accurately evaluate the ultimate capacity and residual deformation, the resistance to compressive stress of the LD bars should be taken into consideration.

Fig. 11(a) also shows the ultimate shear strength calculated by the methods A and B recommended in the guidelines of AIJ [6], represented in purple lines and green lines, respectively. As apparent from Fig. 11(a), both methods underestimated the ultimate shear strength at large deformation for specimen with a shear span ratio of 1.5. Although the calculated results by method B for specimen W20 and W25 were closer to their tested results, it is difficult to discuss the prediction accuracy since no shear failure at the wall panels were observed till the end of the experiments for the specimen with shear span of 2.0 and 2.5.

5. CONCLUSIONS

Three reinforced concrete walls, the longitudinal distributed (LD) bars in the panel of which were not anchored into adjacent beams, were fabricated and tested under reversed cyclic lateral force to investigate the effectiveness of a new arrangement of the LD bars and the influence of shear span ratio on seismic behaviors of concrete walls reinforced by SBPND rebars. Based on the experimental and analytical works described in this paper, the following conclusions can be drawn:

- (1) The utilization of SBPND rebars in the edge zones of wall section could assure RC walls drift-hardening capability up to the drift ratio of 3.0%.
- (2) The new arrangement of LD bars could mitigate the damage of concrete near the wall toes, and prevent the wall with shorter shear span from premature shear failure.
- (3) Current design equations could not give an accurate prediction to the ultimate flexural strength of the walls with SBPND rebars because they do not take account of the slippage of the SBPND rebars.
- (4) The analytical method presented in this paper

could predicted the overall seismic behavior of the RC walls reinforced with SBPND rebars up to large drift with a difference of less than 10% on the conservative side. Comparison with the test results also indicated that the D6 LD bars in the wall panel might resist compressive axial stress at large deformation, increasing the residual drift.

ACKNOWLEDGEMENTS

This study was financially supported by JSPS KAKENHI Grant Number 19H02289. SBPEN rebars were provided by Neturen Co. Ltd. Assistance to the experiment described in this paper by Mr. Kanao, a technical staff of Kobe University is greatly appreciated.

REFERENCES

- [1] Fujitani T. et al. (2018): Effect of the type of concentrated rebars on seismic performance and evaluation of rectangular RC cantilever shear walls, Proceedings of the JCI, 40(2), 313-318, (in Japanese).
- [2] Fukuhara Y. et al. (2018): Study on ductility of reinforced concrete rectangular shear wall with diagonal reinforcement, Proceedings of the JCI, 40(2), 325-330, (in Japanese).
- [3] ICBA. et al. (2015): Commentary on Structural Regulations of the Building Standard Law of Japan, pp.648-695, (in Japanese).
- [4] Sun Y., Sakino K., Yoshioka T. (1996): Flexural behavior of high-strength RC columns confined by rectilinear reinforcement, Journal of Structural and Construction Engineering, Architectural Institute of Japan, No. 486, 95-106.
- [5] Funato Y. et al. (2012): Modeling and application of bond characteristic of HS rebars with spiral grooves, Proceedings of the JCI, 34(2), 157-162, (in Japanese).
- [6] AIJ (1990): Design Guidelines for Earthquake Resistant Reinforced Concrete Buildings Based on Ultimate Strength Concept, p.104, (in Japanese).